Int j simul model 23 (2024) 1, 149-160
Original scientific paper

A CO-SIMULATION MODEL FOR THE OPERATING MECHANISM OF A HIGH-VOLTAGE CIRCUIT BREAKER

Li, X.-F.[*]; Zhao, D.[**]; Yi, L.[***]; Wu, Z.[*]; Zhang, Y.[*] & Shuai, C.-G.[*,#]
[*] College of Power Engineering, Naval University of Engineering, Wuhan, 430072, China
[**] Wuhan Second Ship Design and Research Institute, Wuhan, 430072, China
[***] Department of Operational Research and Programming, Naval University of Engineering, Wuhan, 430072, China
E-Mail: xiaofengli@whu.edu.cn, cgs_whu@163.com ([#] Corresponding author)
Note: Xiaofeng Li and Deng Zhao contributed equally to this work, and are considered as co-first authors.

Abstract
The reliability of high-voltage circuit breakers (HVCBs) depends critically on the dynamic characteristics of their hydraulic operating mechanisms (OMs). However, previous analyses have been limited to discrete components due to the lack of models capturing multi-physics couplings. This paper proposes a novel co-simulation approach for hydraulic OMs that enables system-level analysis. Specifically, the hydraulic system is modelled using the lumped parameter method, and the transmission mechanism is modelled via finite element analysis. The subsystem models exchange inputs and outputs through shared memory, realizing coupling without compromising simulation performance. Experiments on a 550 kV HVCB validate that the model accurately captures OM transient responses. The co-simulation framework has diverse capabilities, including predicting dynamics under varied operating parameters and quantifying stress distributions and response evolution patterns. Overall, this paper proposes an advanced multi-physics analysis capability for hydraulic OMs to support reliability-oriented design and optimization.
(Received in August 2023, accepted in January 2024. This paper was with the authors 2 months for 1 revision.)

Key Words: Operating Mechanisms, Hydraulic System, Transmission Mechanism, Co-Simulation

1. INTRODUCTION

When used as protection and control apparatuses in electric power systems, high-voltage circuit breakers (HVCBs) can complete opening and closing operations in an accurate and timely manner to cut or connect circuits [1]. In general, the operating mechanisms (OMs) of these systems can be classified into spring, motor, electromagnetic and hydraulic types. Among them, hydraulic OMs have the advantages of high power density and stable dynamic performance; thus, they are now widely applied [2]. Hydraulic OMs can be further categorized into hydraulic systems and transmission mechanisms, which are employed for movement and driving load transmission. According to international surveys, OMs are critical for ensuring the operational reliability of HVCBs; approximately 59 % of major operational failures originate from OMs, causing great economic losses [3]. In recent decades, the performance of hydraulic OMs has attracted widespread attention. Many scholars have focused on mechanical fault diagnoses and health assessments based on all types of machine learning and online monitoring techniques [4, 5], which have significantly contributed to improving service reliability. These studies improved the maintenance effectiveness of hydraulic OMs but could not reduce machinery faults from the design source. As performance expectations increase, more effective simulation tools for hydraulic OMs are needed.

With the development of computer-aided engineering (CAE) technology, several numerical simulation methodologies, such as finite element analysis (FEA) [6, 7] and computational fluid dynamics (CFD) [8, 9], have been gradually introduced for the analysis of multibody system dynamics. CAE technology can greatly minimize the number of design reversions and test cycles, hence reducing costs and increasing efficiency. However, independent simulation

methods have been adopted in previous studies for discrete parts of hydraulic OMs. For instance, performance optimizations of the switches, directional valves, and buffer heads of cylinders in hydraulic systems have been reported [10, 11].

Due to the lack of coupling links between a hydraulic system and its transmission mechanism, system-level co-simulation studies are lacking. Independent simulation methods can focus only on the performance of separate hydraulic systems or transmission mechanisms under given kinematic and load boundary conditions. However, without accurate feedback from other coupled subsystems, the dynamic responses of the hydraulic system or transmission mechanism are incomplete. For the hydraulic OM of an HVCB, strong coupling effects generally occur between the fluid and the mechanical structure. The coupling effects of hydraulic–mechanical systems are important for accurate dynamic response analysis, and evaluating the coupling effects requires an overall evaluation of the two subsystems.

The analysis of a hydraulic OM is a typical multi-physics issue involving a hydraulic system and a transmission mechanism. Generally, monolithic and co-simulation approaches have been adopted for multi-physics problems [12, 13]. In a monolithic simulation, an all-encompassing dynamic equation set that describes the behaviour of every component needs to be defined and solved. For instance, using a lumped model, an equation set that describes the responses of the hydraulic system and transmission mechanism can be obtained, and the dynamic behaviour of the whole hydraulic OM system can be solved together as a single matrix system. A monolithic method can be accurate but requires modelling the details of every subsystem, which might be prohibitive for more complicated multi-physics cases.

Co-simulation is another increasingly important methodology that enables complicated multi-physics problems to be solved in parallel mode by several simulation units with data transformation between individual physics solvers [14]. Since it is based on a distributed framework, the advantages of different physics solvers can be fully utilized. In recent decades, co-simulation has received much attention, and a hydraulically actuated mechanism is a particularly interesting case. Considering the effectiveness and stability of a numerical solution, a noniterative co-simulation method was proposed for the mechanical and hydraulic components of a manipulator [15]. In a noniterative co-simulation model, information exchange between subsystems proceeds at selected discrete synchronization points. As the mechanical structure is simplified as a purely rigid subsystem, only the most representative dynamic behaviours can be preserved. Thus, this approach is essentially a reduced-order co-simulation method. Currently, a variety of software packages also consider the system-level multi-physics co-simulation problem. For instance, ANSYS provides a collaborative environment for developing multi-physics solutions, where the dynamic behaviour of a hydraulic system is solved by CFD and the multibody subsystem is determined by FEA simulation [16].

However, the hydraulic system of a hydraulic OM contains a cylinder, multiple valves, and a group of pipelines and joints. Modelling them with a CFD method can be painstaking and prohibitive in terms of computation time. As an alternative, a hydraulic system can be built up in AMESim by the LM due to its high computational efficiency. Notably, AMESim provides an interface program for co-simulation with ADAMS. For example, a remotely operated seabed vehicle was modelled by ADAMS and then integrated into its hydraulic control system under the AMESim environment for co-simulation [17]. However, in that co-simulation case, the mechanical simulation model worked as the slave machine of the hydraulic system; thus, the model needed to be compiled into an executable submodel and then integrated into the AMESim environment. To achieve this, the mechanical part is generally simplified as a rigid body system. For a hydraulic OM, the operation process is designed to be on the order of 10 ms. Under those circumstances, the flow in the hydraulic system is characterized by high pressure and a large rate, which eventually affect the nonlinear dynamic responses of the transmission mechanism [18].

On the other hand, under high-speed conditions, flexible flow can cause vibration in the transmission mechanism and further feed back to the hydraulic system. Comparisons among the rigid mechanical structures produced by the reduced-order method and their flexible counterparts obtained via FEA can be found in previous studies [19, 20]. It was reported that neglecting the flexibility of the transmission mechanism will introduce large analysis errors to the dynamic response analysis of a hydraulic OM; thus, the FEA method is suggested for modelling the transmission mechanism. For the hydraulic system, the detailed flow distribution is not considered in the hydraulic OM co-simulation model; thus, the fluid dynamics solver AMESim is considered for model building. To achieve co-simulation, different subsystems running in individual physics solvers during different processes need to communicate with each other. As the individual solvers cannot directly interact with each other, a computational co-simulation framework is designed to manage the simulation process.

To our knowledge, this novel co-simulation method is investigated for the first time, providing a useful and unique tool for analysing the performance of hydraulic OMs in optimization and new product design cases. More specifically, a co-simulation approach was innovatively developed to build coupling links for a hydraulic OM. The application of the co-simulation model captures the dynamic responses of the hydraulic OM and obtains a system-level optimization scheme. The remainder of the paper is organized as follows. Section 2 describes the hydraulic OM of an HVCB. Section 3 outlines the simulation model of the studied hydraulic OM and then describes the co-simulation framework. The experimental validations and model applications are described in Section 4. Finally, the conclusions of this study are drawn in Section 5.

2. HYDRAULIC SYSTEM PRINCIPLES

A schematic diagram of the hydraulic OM used in this study is shown in Fig. 1. It generally consists of a hydraulic system (components 1 to 7) and a transmission mechanism (components 8 to 16). Working as the executive component of the hydraulic system, valve-controlled cylinder 7 is connected with pushing link 8 of the transmission mechanism. In brief, the hydraulic OM operations of the HVCB involve touching and separating the master and slave contacts, which correspond to the closing and opening operations of the circuit, respectively.

Supply port P in the hydraulic system is connected to high-pressure oil, and port T is connected to the oil tank. In the initial state, two pilot valves and secondary valves are closed. For the closing operation, high-speed solenoid 1.1 is first energized, and the spool is lifted to open pilot valve 2.1. Then, chamber Cs1 connects with port T and decreases its pressure. As the oil pressure in chamber Cs1 decreases, the spool of secondary valve 3.1 is raised by its inner spring to connect chamber A and chamber B. Second, the opening of secondary valve 3.1 quickly increases the pressure in chamber Cm and pushes the main spool leftward. Then, port P connects to the cylinder to inject high-pressure oil to drive the closing operation.

On the other hand, for the opening operation, once the high-speed solenoid is energized, pilot valve 2.2 connects chamber Cs2 with port T to decrease its chamber pressure. Then, the secondary valve is raised to connect chamber A with chamber B. As secondary valve 3.2 opens, the pressure in chamber Cm decreases promptly due to the large flow into port T. Therefore, the main spool moves rightwards, and the cylinder is connected to port T. As a result, the piston rod performs backwards movement to complete the opening operation. The transmission mechanism is a set of multilink articulated mechanical systems. Notably, compression chamber 9, master contact 10, and nozzle 12 are fixedly connected. Nozzle 12 is articulated with two nozzle links, and arc-extinguishing chamber 13 is articulated with two chamber links 15. Driven by the hydraulic system, the master and slave contacts keep moving in opposite directions to complete the circuit closing or opening operation.

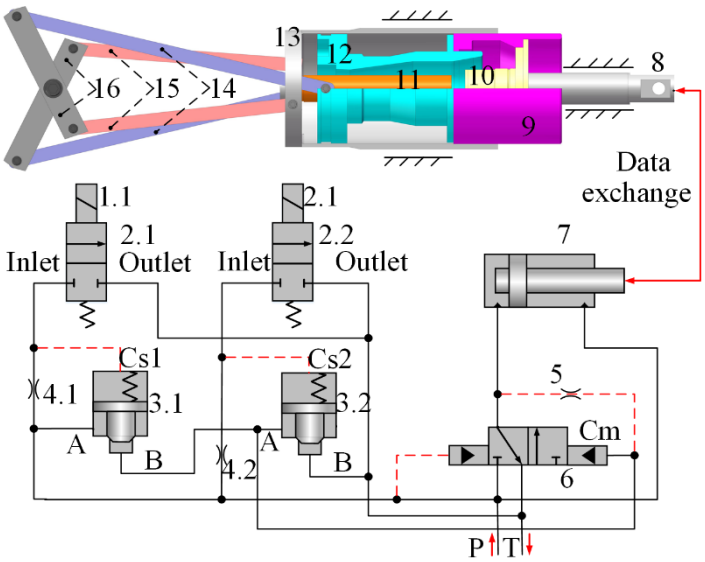

1. High-speed solenoid
2. Pilot valves
3. Secondary valves
4. Secondary valve control orifices
5. Main valve control orifice
6. Main valve
7. Cylinder
8. Pushing link
9. Compression chamber
10. Master contact
11. Slave contact
12. Nozzle
13. Arc-extinguishing chamber
14. Nozzle link
15. Chamber link
16. Middle link

Figure 1: Schematic diagram of a hydraulic OM.

3. RESEARCH METHODOLOGY

3.1 Modelling of the hydraulic system

The hydraulic system mainly consists of pilot valves with high-speed solenoids, two secondary valves, one main valve, one cylinder, and complicated pipelines, which introduce many governing equations. It would be quite time-consuming to perform CFD analysis for the hydraulic system, and nonconvergence could easily occur. The lumped model can produce more comprehensive results while ignoring the details of the flow field; thus, it runs quickly.

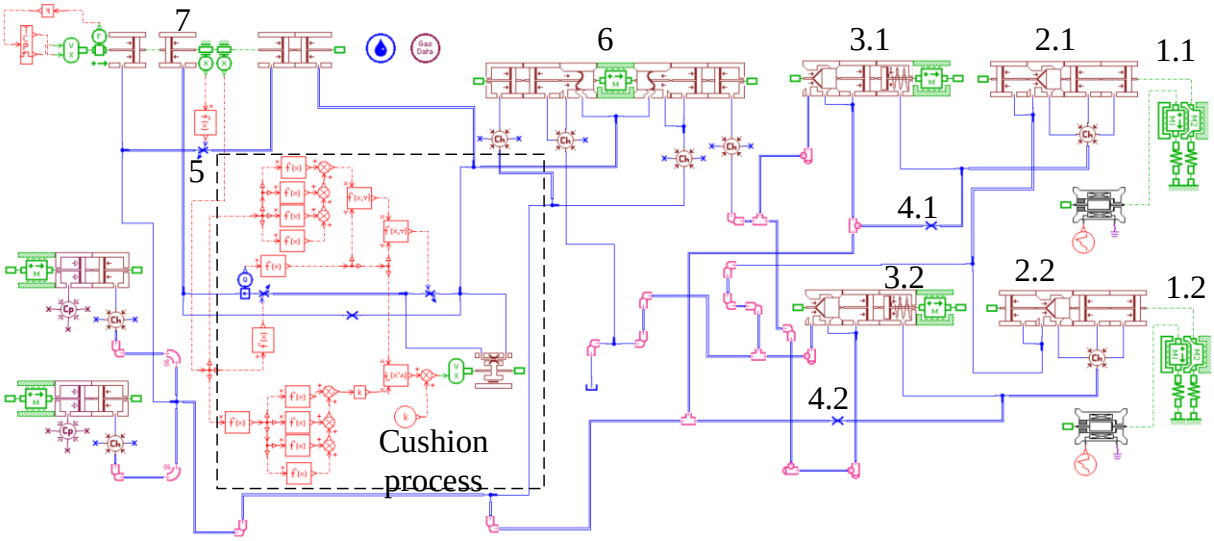

Figure 2: Lumped model of the hydraulic system.

As shown in Fig. 2, a dynamic simulation model of the hydraulic system is established by the lumped model with the AMESim software platform. For the cylinder, an inside multistep cushion is applied for impact suppression, which greatly affects the motion of the transmission mechanism. Since a multistep structure is adopted in the cushion plunger, it cannot be modelled by the standard hydraulic components in the AMESim library. The cushioning process in the cylinder is phased, the dynamic equation of which changes with the displacement of the rod in the cylinder; the related modelling of the cushioning process is given below.

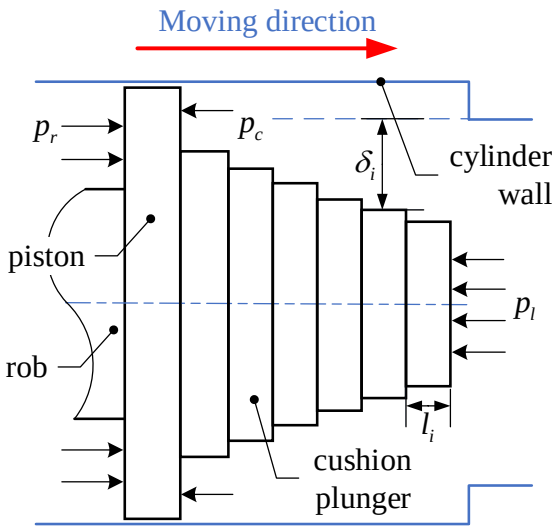

Figure 3: Cushion plunger of the cylinder and its cushioning process.

Fig. 3 describes the main structure of the cushion plunger of the cylinder and its cushioning process. A nonstandard structure is adopted in the cushion plunger, which makes the flow field of the cushioning process complex. To accurately express the flow dynamics in the cushioning process, the fluid dynamics equation can be divided into three stages [13], namely, cylindrical throttling, cone throttling, and torus throttling. In cylindrical throttling, the plunger is far from the inner convex surface of the cylinder wall, in which the flow channel section suddenly shrinks, resulting in local pressure loss. The flow rate in this stage can be expressed as follows:

$$Q_{c1} = C_f \frac{\pi d^2}{4} \sqrt{\frac{2}{\rho_o}(p_c - p_l)} \tag{1}$$

where Q_{c1} is the flow rate during the cylindrical throttling process, C_f is the flow coefficient, d is the inner diameter of the cushion hole, and p_c and p_l represent the differences between the pressure values determined before and after the flow passage area reduction step, respectively. Here, ρ_o is the oil density. As the plunger moves rightwards and approaches the convex surface of the cylinder wall, a sharp-edged orifice restriction can be used to describe the fluid dynamics in the cone throttling process:

$$Q_{c2} = C_f d\pi \sqrt{(l_0 - x)^2 + \delta^2} \sqrt{\frac{2}{\rho}(p_c - p_l)} \tag{2}$$

where Q_{c2} is the flow rate during the cone throttling process, l_0 is the initial distance between the plunger and cushion hole at the beginning of the cushioning process, x is the plunger displacement, and δ demonstrates the annular gap of the plunger step. When the plunger enters the cushion hole, torus throttling occurs, and the corresponding flow rate equation is generally defined as follows:

$$Q_{c3} = d\pi \left[\frac{(p_c - p_l)\delta^3}{12\mu(x - l_0)} + \frac{\delta v}{2} \right] \tag{3}$$

where Q_{c3} is the flow rate during the torus throttling process, μ is the dynamic viscosity of the oil, and **v** is the movement speed of the piston. The cylinder model is programmed to set up a submodel by taking its inside cushioning process into account. The other valves can be completed with the standard submodel provided by the hydraulic component library in AMESim and then connected by its pipelines.

3.2 Modelling of the hydraulic system

Owing to the high speeds and heavy loads, the dynamic responses of the transmission mechanism are strongly affected by the flexibility levels of the parts. Alternate elastic deformation and recovery occur in the transmission mechanism, which damages the movement accuracy and reduces the service life of the hydraulic OM. Compared with that of the rigid model, the synthesis of FEA into co-simulation permits the analysis of the detailed stress distribution of the transmission mechanism, which is useful in the design process of a hydraulic OM. Therefore, mechanical flexibility is essential in the co-simulation modelling process.

In this case, the FEA method is employed for modelling the transmission mechanism. Considering the structural complexity of the transmission mechanism, related meshing work is carried out in HyperMesh, in which three key steps are involved, namely, geometry preparation, attribute setting, and mesh generation. In the geometry preparation process, the three-dimensional components are first imported into HyperMesh software, after which model scale selection, necessary geometric simplification, topology repair, and structure segmentation are performed. Afterwards, the material properties, boundary conditions, simulation parameter settings, and data interaction surface are determined during the attribute setting steps. Finally, the mesh type and division method are determined in the mesh generation step, and the simulation solution file is exported to LS-DYNA.

Structural meshing is important for realizing improved simulation accuracy and efficiency while analysing the dynamic transmission mechanism via the FEA method. In general, smaller elements indicate higher simulation calculation accuracy but longer computer running times. In addition, high-quality structured mesh types such as hexahedrons can achieve better convergence and computational efficiency than can their unstructured counterparts such as tetrahedrons, but they also increase the difficulty of the structural meshing process. Therefore, the structure mesh generation step is a critical multiobjective trade-off process. The final FEA model produced under LS-DYNA R8.0 for the transmission mechanism is shown in Fig. 4.

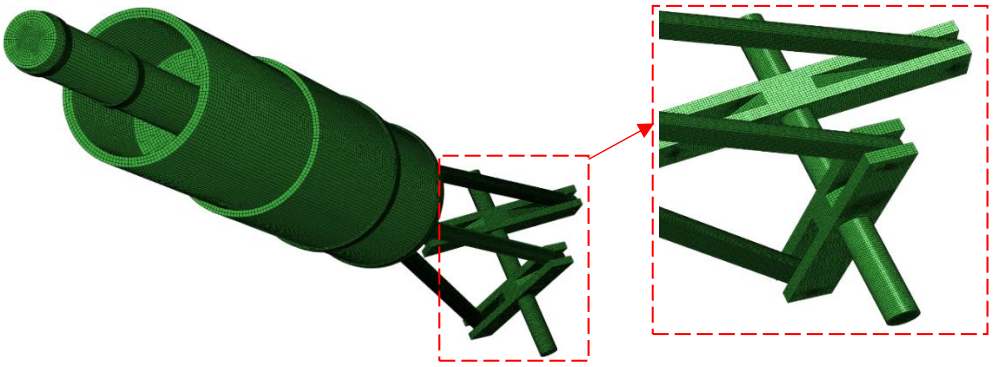

Figure 4: FEA model of the transmission mechanism.

According to Fig. 4, for the sake of accuracy and efficiency, enough hexahedral elements are first utilized to discretize the components of the transmission mechanism. At least three layers of elements in the thickness direction of the rod parts should be ensured. Additionally, for most complicated parts, such as the middle link in Fig. 1, hybrid tetrahedral and hexahedral meshes are considered for meshing. After verifying the element size independence, the whole transmission mechanism is divided into a total of 1.2 million elements.

3.3 Coupling of the co-simulation model

As outlined in Fig. 5, the co-simulation framework in this work is based on shared memory and parallel distribution, ensuring the efficiency and stability of the simulation process without compromising the overall simulation performance [16]. The co-simulation framework contains

three input–output variables between different simulation models and shared memory. A total of four shared memory areas are developed for data interaction and identifier conversion.

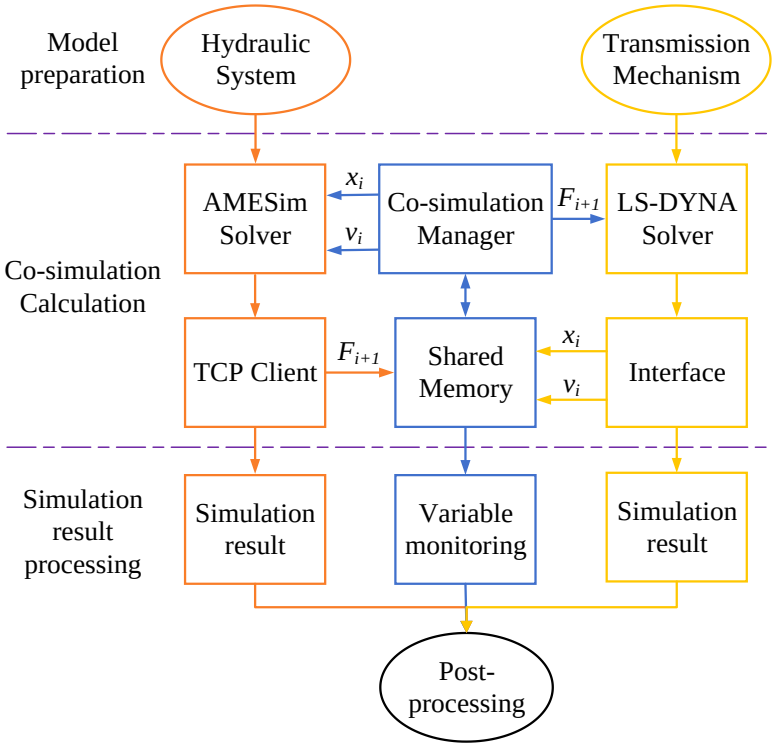

Figure 5: Co-simulation framework of the hydraulic OM.

As co-simulation is executed in the parallel distribution mode with two spawned solver processes, communication for the different simulation control processes and the coupling of data transfers between different subsystem solvers are indispensable. To achieve communication between the shared memory and hydraulic system, a TCP/IP-based client–server infrastructure is adopted. In this case, the TCP/IP communication module is developed and added to the simulation model of the hydraulic system and subsequently set as a server. In one co-simulation step, the identifier value in the shared memory is initially set as a positive state, and the hydraulic system model is first activated. When one simulation step of the hydraulic system is completed, the TCP module accesses the preset shared memory to write the obtained hydraulic force and read the displacement and velocity of the master contact. Then, the identifier is switched to a negative state, and the hydraulic system simulation is suspended. In this process, the dynamic solver of the transmission mechanism is suspended but keeps accessing the identifier.

The communication between the shared memory and the FEA solver of the transmission mechanism involves the secondary development of the application programming interfaces of the software, which is related mainly to the modification of LS_DYNA communication files. First, the subroutine program is rewritten to add functions for accessing shared memory, reading, and resetting the boundary conditions of the coupling surface. The amended communication files are subsequently recompiled for co-simulation. When the identifier value is converted to a negative state, the LS_DYNA solver is activated via remote procedure calls. Similar to the simulation of the hydraulic system, the displacement and velocity after one simulation step are written to the shared memory, and the solver reads the hydraulic force for the next simulation step. Afterwards, the identifier in the shared memory is reset to a positive state to complete one co-simulation step. This cycle continues until the end of the whole co-simulation process. The coupling setting is arranged between the pushing link and the cylinder

(refer to Fig. 1). During co-simulation, the driving force from the cylinder is transformed to the pushing link for the operating/closing operation. On the other hand, the inertia and resistance from the transmission mechanism are loaded to the hydraulic system through the cylinder. Considering stability/accuracy, the frequency of interaction between different subsystems is relatively high (1.1×10^7 Hz), and the communication interval is approximately 0.0002 % of the total co-simulation time (40 milliseconds).

4. RESULTS AND DISCUSSION

4.1 Experimental verification

Based on the developed dynamic simulation model for each subsystem and the proposed coupling method, a system-level co-simulation model of a hydraulic OM is established. The co-simulation model is executed on a Windows 10 machine with a 64-bit operating system and an Intel Xeon CPU at 3.2 GHz (16 cores) with 256 GB of RAM. The total co-simulation time is 40 ms, which requires approximately 32 h of absolute wall-clock time to run, and the communication intervals between different subsystems are 8.5×10^{-8} s. In addition, the displacement is measured via an operating experiment and compared with the corresponding numerical results to verify the performance of the co-simulation model.

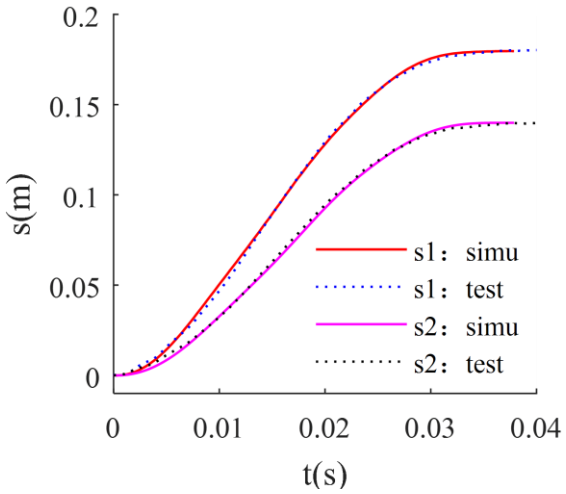

Figure 6: The variations in the measured displacements and their co-simulated results versus time.

In general, a high voltage and an overheated electric arc form between the two main contacts of the HVCB during its opening process. A longer completion time for the opening operation prolongs the breakdown of the filling medium and eventually increases the risk of contact welding. Therefore, HVCB opening needs to be completed in tens of milliseconds. On the other hand, an overly fast opening operation also leads to a great structural strength challenge and promotes machinery faults in the transmission mechanism. Therefore, the displacement curves on the hydraulic system side (the pushing link in Fig. 1) and the final execution side (the slave contact in Fig. 1) during the opening operation are critical and must obey very strict timing standards. In this section, the measured displacements and their co-simulated counterparts are displayed in Fig. 6.

In the figure, “s1” denotes the displacement–time curve of the master contact, and “s2” denotes that of the slave contact. The travel curves of both the pushing link and slave contact from the co-simulation model agree well with the experimental data. The movement times of the two contacts obtained from the co-simulation and experimental data were 3.6×10^{-2} s and 3.8×10^{-2} s, respectively, with an error of only 2×10^{-3} s, which effectively verified the accuracy of the co-simulation model. The simulated opening completion time is slightly shorter than that

of the test, which can be explained by the time-varying oil viscosity and insufficient lubrication of the mechanism system under the experimental conditions.

4.2 Model application

The aim of co-simulating a hydraulic OM is to shorten product development cycles and reduce the costs associated with the testing, validation, and redesign of OM prototypes. Consequently, the established co-simulation model should permit the quantification of important system operation features. In this section, based on the co-simulation model, the stress distributions of several key parts of the transmission mechanism and the operation predictions produced under different main parameters are analysed to illustrate its capabilities. Compared with that of the lumped multibody system, the modelling process of the transmission mechanism in our co-simulation model is based on FEA. Thus, this approach enables detailed stress analysis, which is useful for structural optimization and intensity checks of mechanical systems. For instance, Fig. 7 shows the corresponding stress results of the nozzle link, chamber link, and middle link in the transmission mechanism obtained from co-simulation under the opening operation.

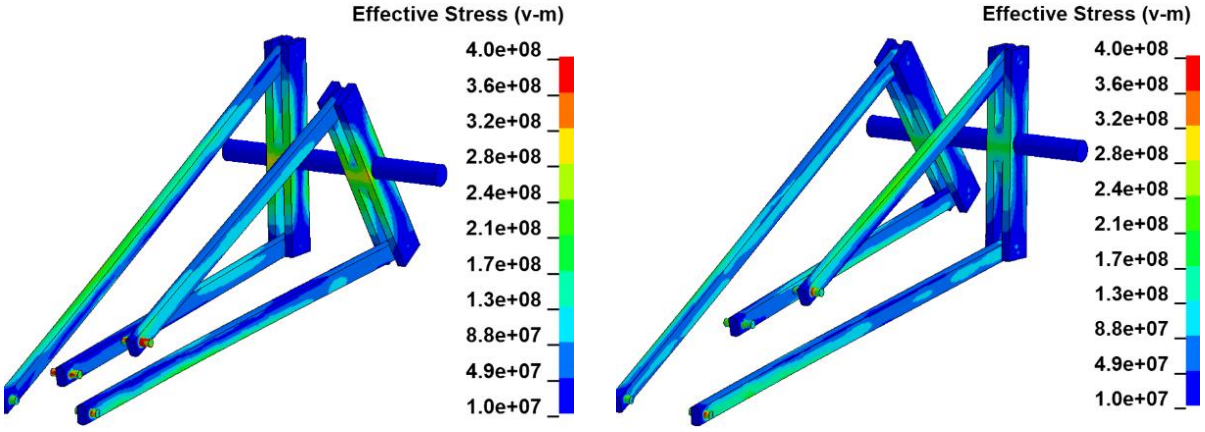

a) t = 0,01 s b) t = 0,02 s

Figure 7: Stress distribution analysis of the opening operation.

Fig. 7 shows that the average stress in the nozzle link is the highest among the three components. In addition, a visible local stress concentration appears in the revolute joint. The local stress on the journal can reach 389 MPa, where severe wear would be generated and develop during the service of the HVCB. Based on the aforementioned stress analysis via co-simulation, further structure optimization suggestions can be proposed. For example, shape topology optimization research focused on vibration reduction should be applied to transmission mechanisms in future. Furthermore, the stress concentration in the revolute joint is sensitive to the bearing hole diameter, shaft length, and joint clearance size. Therefore, the Taguchi method is also recommended for multifactor optimization designs aimed at weakening the stress concentration.

The input high-pressure oil provides the mechanical energy for the closing and opening operations of the HVCB; thus, the initial oil pressure strongly affects the dynamic outputs of the transmission mechanism. A higher pressure accelerates the movement of the two main contacts to reduce the operation time but also imposes a greater dynamic load on the transmission mechanism and inevitably increases the pressure fluctuations in the hydraulic system. Additionally, oil leakage and severe vibration responses always occur under high-pressure operating conditions. A balance needs to be achieved between fast operation and performance stability. Therefore, the operation predictions obtained under different initial oil pressures of the accumulator are meaningful, especially in the new prototype hydraulic OM

design, since they can guide the structural optimization and operational testing of hydraulic OMs.

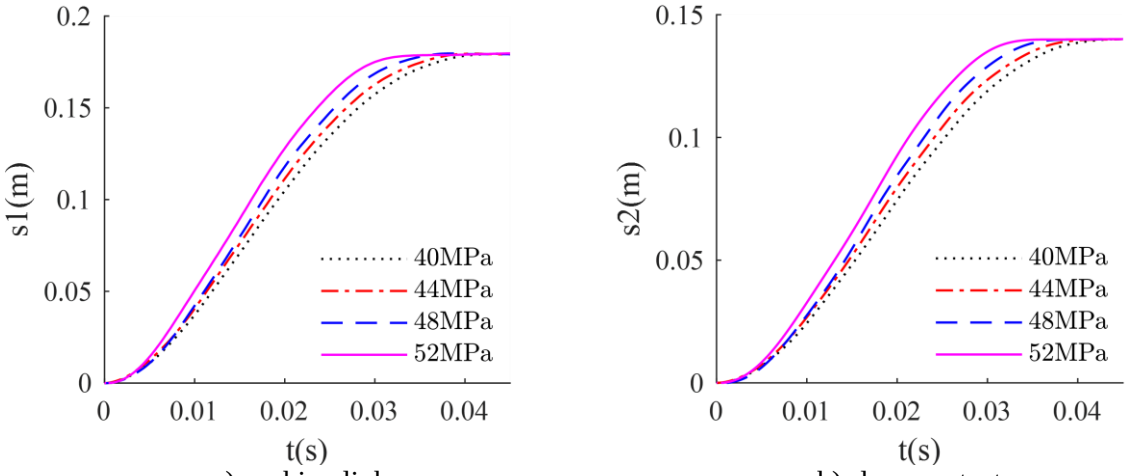

a) pushing link b) slave contact

Figure 8: Displacement predictions for the opening operation.

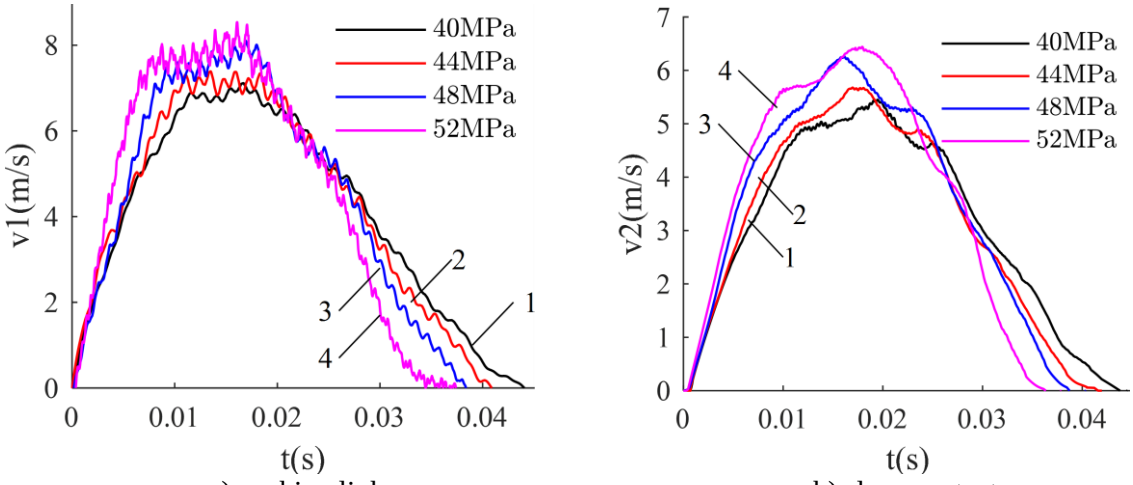

a) pushing link b) slave contact

Figure 9: Velocity predictions for the opening operation.

Figs. 8 and 9 show that within the studied oil pressure range, stable displacement outputs can be obtained, and the displacement stroke of the hydraulic OM remains constant. After the opening operation, the total relative displacement between the two contacts is 0.32 m, of which 0.18 m is contributed by the master contact and 0.14 m is contributed by the slave contact. As expected, the opening time is shortened as the initial oil pressure increases.

On the one hand, obvious fluctuations can be detected in the input velocity curve of the pushing link, and the fluctuation amplitude and oil pressure are positively correlated. This suggests an unstable hydraulic force from the hydraulic system and a nonlinear axial vibration output from the hydraulic OM. To improve the operational stability, the current cushion structure inside the cylinder needs further optimization. On the other hand, the velocity responses of the slave contact are more stable, indicating that the flexible transmission mechanism has a buffering effect on suppressing vibration. Notably, a 7×10^{-4} s delay appears in the start-up of the slave contact, which can be attributed to the elastic deformation accumulation processes of flexible parts. Finally, a good compromise between fast responses and stable performance outputs seems to be achieved when the oil pressure improves from 44 MPa to 48 MPa since obvious time shortening can be achieved with a slight velocity

fluctuation increase while the oil pressure rises. A further investigation of the multiobjective parameter optimization process of hydraulic OM will be conducted through co-simulation in the future.

5. CONCLUSION

For the multi-physics analysis of the hydraulic OM of an HVCB, a distributed parallel-mode co-simulation model concerning fluid–mechanical coupling effects is presented for the first time, providing designers with a more systematic perspective level to quantify hydraulic OM behaviours. The main steps can be summarized as follows: 1) A TCP/IP-based client–server infrastructure is adopted in a lumped model of the hydraulic system under AMESim, and interface development is conducted in a FEA model of the transmission mechanism under LS_DYNA. 2) A co-simulation management approach is developed to control the simulation process, in which data transfer between different physic solvers is realized through variable exchange with shared memory. 3) The stress evolution process can be obtained by the co-simulation model. In addition, a good compromise between fast responses and stable performance outputs can be achieved for a hydraulic OM when the oil pressure increases from 44 MPa to 48 MPa.

In summary, the reported co-simulation method provides a novel tool for analysing the main performance parameters and permits the prediction of the dynamic evolution process of the hydraulic OM of an HVCB with a reduced need for physical prototyping. Further optimization analysis of a hydraulic OM based on a co-simulation model should be conducted in future work.

ACKNOWLEDGEMENT

This work was supported by Postdoctoral Fellowship Program of CPSF (grant number GZC20233550).

REFERENCES

[1] Liu, Y.; Zhang, G.; Zhao, C.; Qin, H.; Yang, J. (2021). Influence of mechanical faults on electrical resistance in high voltage circuit breaker, *International Journal of Electrical Power & Energy Systems*, Vol. 129, Paper 106827, 10 pages, doi:10.1016/j.ijepes.2021.106827

[2] Li, X.; Zheng, X.; Zhang, T.; Guo, W.; Wu, Z. (2023). Robust fault diagnosis of a high-voltage circuit breaker via an ensemble echo state network with evidence fusion, *Complex & Intelligent Systems*, Vol. 9, No. 5, 5991-6007, doi:10.1007/s40747-023-01025-3

[3] Razi-Kazemi, A. A.; Niayesh, K. (2020). Condition monitoring of high voltage circuit breakers: past to future, *IEEE Transactions on Power Delivery*, Vol. 36, No. 2, 740-750, doi:10.1109/TPWRD.2020.2991234

[4] Yao, Y.; Wang, N. (2020). Fault diagnosis model of adaptive miniature circuit breaker based on fractal theory and probabilistic neural network, *Mechanical Systems and Signal Processing*, Vol. 142, Paper 106772, 9 pages, doi:10.1016/j.ymssp.2020.106772

[5] Gao, W.; Qiao, S.-P.; Wai, R.-J.; Guo, M.-F. (2021). A newly designed diagnostic method for mechanical faults of high-voltage circuit breakers via SSAE and IELM, *IEEE Transactions on Instrumentation and Measurement*, Vol. 70, Paper 3500613, 13 pages, doi:10.1109/TIM.2020.3011734

[6] Plavec, E.; Filipović-Grčić, B.; Vidović, M. (2020). The impact of plunger angle and radius on the force and time response of DC solenoid electromagnetic actuator used in high-voltage circuit breaker, *International Journal of Electrical Power & Energy Systems*, Vol. 118, Paper 105767, 7 pages, doi:10.1016/j.ijepes.2019.105767

[7] Zeng, G.; Yang, X.; Yin, H.; Jing, Y.; Zhao, S.; Cao, J. (2020). Unsymmetrical bistable multimagnetic circuit permanent magnet actuator for high-voltage circuit breaker application: analysis, design, and dynamic simulation, *IET Electric Power Applications*, Vol. 14, No. 5, 827-836, doi:10.1049/iet-epa.2019.0559

[8] Fu, S.; Guo, X. Y.; Dong, L. H.; Sheng, K.; Sun, A. (2022). Numerical simulation of migration laws of dense particle flow in pipelines, *International Journal of Simulation Modelling*, Vol. 21, No. 1, 89-100, doi:10.2507/IJSIMM21-1-592

[9] Zhao, L.; Li, Y. (2023). Wind load of low-rise building based on fluent equilibrium atmospheric boundary layer, *Technical Gazette*, Vol. 30, No. 4, 1274-1282, doi:10.17559/TV-20230205000324

[10] Smajkic, A.; Bosovic Hadzovic, B.; Muratovic, M.; Kim, M. H.; Kapetanovic, M. (2020). Determination of discharge coefficients for valves of high voltage circuit breakers, *IEEE Transactions on Power Delivery*, Vol. 35, No. 3, 1278-1284, doi:10.1109/TPWRD.2019.2939746

[11] Zhong, Q.; Bao, H.; Li, Y.; Hong, H.; Zhang, B.; Yang, H. (2021). Investigation into the independent metering control performance of a twin spools valve with switching technology-controlled pilot stage, *Chinese Journal of Mechanical Engineering*, Vol. 34, Paper 91, 17 pages, doi:10.1186/s10033-021-00616-w

[12] Rahikainen, J.; Mikkola, A.; Sopanen, J.; Gerstmayr, J. (2018). Combined semi-recursive formulation and lumped fluid method for monolithic simulation of multibody and hydraulic dynamics, *Multibody System Dynamics*, Vol. 44, No. 3, 293-311, doi:10.1007/s11044-018-9631-x

[13] Xu, B.; Ding, R.; Zhang, J.; Sha, L.; Cheng, M. (2016). Multiphysics-coupled modeling: simulation of the hydraulic-operating mechanism for a SF6 high-voltage circuit breaker, *IEEE/ASME Transactions on Mechatronics*, Vol. 21, No. 1, 379-393, doi:10.1109/TMECH.2015.2460351

[14] Gomes, C.; Thule, C.; Broman, D.; Larsen, P. G.; Vangheluwe, H. (2018). Co-simulation: a survey, *ACM Computing Surveys*, Vol. 51, No. 3, Paper 49, 33 pages, doi:10.1145/3179993

[15] Rahikainen, J.; González, F.; Naya, M. Á.; Sopanen, J.; Mikkola, A. (2020). On the cosimulation of multibody systems and hydraulic dynamics, *Multibody System Dynamics*, Vol. 50, No. 2, 143-167, doi:10.1007/s11044-020-09727-z

[16] Chimakurthi, S. K.; Reuss, S.; Tooley, M.; Scampoli, S. (2018). ANSYS workbench system coupling: a state-of-the-art computational framework for analyzing multiphysics problems, *Engineering with Computers*, Vol. 34, 385-411, doi:10.1007/s00366-017-0548-4

[17] Dai, Y.; Zhu, X.; Chen, L. S. (2016). A mechanical-hydraulic virtual prototype co-simulation model for a seabed remotely operated vehicle, *International Journal of Simulation Modelling*, Vol. 15, No. 3, 532-541, doi:10.2507/IJSIMM15(3)CO11

[18] Yang, Q.; Ruan, J.; Zhuang, Z.; Huang, D. (2020). Chaotic analysis and feature extraction of vibration signals from power circuit breakers, *IEEE Transactions on Power Delivery*, Vol. 35, No. 3, 1124-1135, doi:10.1109/TPWRD.2019.2934123

[19] Masovic, R.; Breski, T.; Cular, I.; Vuckovic, K.; Zezelj, D. (2021). Numerical model for worm gear pair inspection based on 3D scanned data, *International Journal of Simulation Modelling*, Vol. 20, No. 4, 637-648, doi:10.2507/IJSIMM20-4-573

[20] Li, Y.; Wang, Z.; Chen, C.; Xu, T.; Chen, B. (2022). Dynamic accuracy analysis of a 5PSS/UPU parallel mechanism based on rigid-flexible coupled modeling, *Chinese Journal of Mechanical Engineering*, Vol. 35, Paper 33, 14 pages, doi:10.1186/s10033-022-00693-5